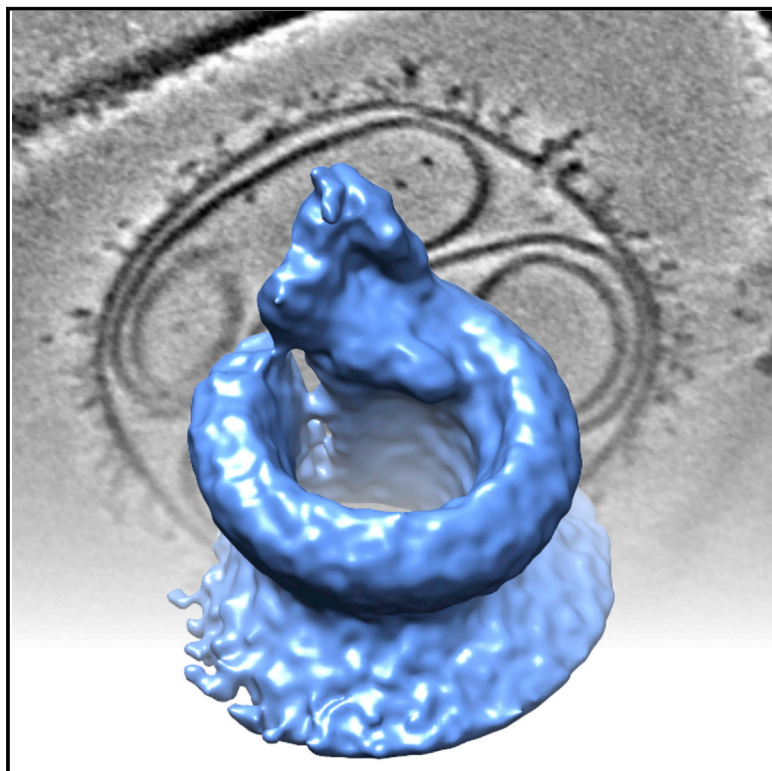


Cell Reports

Heterogeneous MAC Initiator and Pore Structures in a Lipid Bilayer by Phase-Plate Cryo-electron Tomography

Graphical Abstract



Authors

Thomas H. Sharp, Abraham J. Koster, Piet Gros

Correspondence

t.sharp@lumc.nl (T.H.S.),
p.gros@uu.nl (P.G.)

In Brief

Immune defense by complement forms membrane attack complex pores in membranes. Using phase-plate cryo-electron tomography, Sharp et al. find heterogeneous oligomeric MAC structures in membranes. Subtomogram averaging of single pores at 2.3-nm resolution reveals a cone-shaped, twisted barrel that is incompletely closed.

Highlights

- MAC pores are cone shaped, twisted, and poorly sealed between C9 end and C5b-8 start
- Complement activation yields single and joined MAC pores in lipid membranes
- Oligomerization of three to four C5b-8 complexes causes ~3.5-nm pores in membranes
- Phase plates markedly increase interpretability of cryo-electron tomograms



Sharp et al., 2016, Cell Reports 15, 1–8
April 5, 2016 ©2016 The Authors
<http://dx.doi.org/10.1016/j.celrep.2016.03.002>

CellPress

Heterogeneous MAC Initiator and Pore Structures in a Lipid Bilayer by Phase-Plate Cryo-electron Tomography

Thomas H. Sharp,^{1,*} Abraham J. Koster,^{1,2} and Piet Gros^{3,*}

¹Section Electron Microscopy, Department of Molecular Cell Biology, Leiden University Medical Center, 2300 RC Leiden, the Netherlands

²NeCEN, Gorlaeus Laboratories, Leiden University, 2333 CC Leiden, the Netherlands

³Crystal and Structural Chemistry, Bijvoet Center for Biomolecular Research and Department of Chemistry, Faculty of Science, Utrecht University, Padualaan 8, 3584 CH Utrecht, the Netherlands

*Correspondence: t.sharp@lumc.nl (T.H.S.), p.gros@uu.nl (P.G.)

<http://dx.doi.org/10.1016/j.celrep.2016.03.002>

SUMMARY

Pore formation in membranes is important for mammalian immune defense against invading bacteria. Induced by complement activation, the membrane attack complex (MAC) forms through sequential binding and membrane insertion of C5b6, C7, C8, and C9. Using cryo-electron tomography with a Volta phase plate and subtomogram averaging, we imaged C5b-7, C5b-8, and C5b-9 complexes and determined the C5b-9 pore structure in lipid bilayers. The in situ C5b-9 pore structure at 2.3-nm resolution reveals a 10- to 11.5-nm cone-shaped pore starting with C5b678 and multiple copies of C9 that is poorly closed, yielding a seam between C9 and C6 substituting for the shorter β strands in C6 and C7. However, large variations of composite pore complexes are apparent in subtomograms. Oligomerized initiator complexes C5b-7 and C5b-8 show stages of membrane binding, deformation, and perforation that yield ~ 3.5 -nm-wide pores. These data indicate a dynamic process of pore formation that likely adapts to biological membranes under attack.

INTRODUCTION

Activation of the mammalian complement system induces formation of membrane attack complexes (MACs), yielding pores in membranes of invading microbes (see, e.g., [Ricklin et al., 2010](#)). MAC formation is critical for human defense against gram-negative bacteria of the *Neisseria* genus ([Stephens et al., 2007](#)). However, host cells are also vulnerable to MAC, as is apparent in paroxysmal nocturnal hemoglobinuria and atypical hemolytic uremic syndrome ([Noris and Remuzzi, 2009](#); [Parker, 2007](#)). In recent years, awareness has grown that complement activation and MAC formation may impound on many disease pathogenesises that involve tissue maintenance, with various tissues affected, such as brain, heart, kidney, eyes, and teeth gums (see, e.g., [Morgan and Harris, 2015](#); [Ricklin et al., 2010](#)).

MAC formation starts when C5 convertases cleave C5 into C5a and C5b ([Müller-Eberhard, 1986](#)). Upon production, C5b associates with C6, forming the soluble C5b6 complex ([Cooper and Müller-Eberhard, 1970](#)). Addition of C7 generates C5b67, denoted as C5b-7, which adheres to membranes ([DiScipio et al., 1988](#); [Preissner et al., 1985](#)). Association of the heterotrimeric C8 $\alpha\beta\gamma$ yields C5b-8, which forms small pores with a 0.9-nm diameter and, as time progresses, generates 3-nm pores ([Ramm et al., 1982](#); [Zalman and Müller-Eberhard, 1990](#)). In normal human sera (NHS), C5b-9 creates ~ 10 -nm pores ([Tschopp, 1984](#)). Negative-stain electron microscopy studies in the 1980s provided low-resolution images of C5b-7 ([DiScipio et al., 1988](#); [Preissner et al., 1985](#)), C5b-8 ([Bhakdi and Tranum-Jensen, 1984](#); [Podack et al., 1982](#)), and C5b-9 ([Tschopp, 1984](#)). Crystal structures of C5 ([Fredslund et al., 2008](#)), C6 ([Aleshin et al., 2012b](#)), and C8 $\alpha\beta\gamma$ ([Lovelace et al., 2011](#)) and the first MAC-initiating complex, C5b6 ([Aleshin et al., 2012a](#); [Hadders et al., 2012](#)), gave insights into structural details. Structures of MAC-perforin (MACPF) domains of C8 α ([Hadders et al., 2007](#)) and Plu-MACPF from *P. luminescens* ([Rosado et al., 2007](#)) suggested a mechanistic resemblance to bacterial cholesterol-dependent cytolysins (CDCs), in which loosely folded α helices rearrange into transmembrane β -hairpins that extend from the kinked β strands, forming a β -barrel pore ([Shatursky et al., 1999](#); [Shepard et al., 1998](#)). For the CDC perfringolysin, formation of pre-pore complexes on top of the membrane before membrane perforation was observed ([Hotze et al., 2001](#)). In contrast, half- or hemi-pores were posited for MAC formation ([Bhakdi and Tranum-Jensen, 1984](#)) and recently proposed to exist for CDC pneumolysin ([Sonnen et al., 2014](#)). Atomic-force microscopy studies confirm formation of these seemingly unfavorable membrane structures for CDC suilyisin in phosphatidylcholine:cholesterol membranes ([Leung et al., 2014](#)).

Advances in cryo-electron tomography (cryo-ET; [Asano et al., 2016](#); [Nogales and Scheres, 2015](#)) facilitate reinvestigations of in situ MAC formation in lipid bilayers. We took advantage of a Volta phase plate ([Danev et al., 2014](#)) installed on a Titan Krios transmission electron microscope with a Falcon II direct electron detector. This setup significantly improves the contrast at low resolution, which markedly increases the interpretability of tomographic volumes collected in focus ([Fukuda et al., 2015](#)) and

Download English Version:

<https://daneshyari.com/en/article/2040125>

Download Persian Version:

<https://daneshyari.com/article/2040125>

[Daneshyari.com](https://daneshyari.com)